



# Callose synthase family genes plays an important role in the *Citrus* defense response to *Candidatus Liberibacter asiaticus*

Lais Moreira Granato · Diogo Manzano Galdeano ·  
Nathália Da Roz D'Alessandre ·  
Michèle Claire Breton · Marcos Antonio Machado

Accepted: 15 April 2019 / Published online: 3 May 2019  
© The Author(s) 2019

**Abstract** Huanglongbing (HLB) is a destructive disease of citrus. The disease is caused by the phloem-limited fastidious proteobacterium *Candidatus Liberibacter asiaticus*, which is transmitted by the Asian citrus psyllid (*Diaphorina citri*). The symptoms of HLB have been related by callose accumulation in the phloem sieve plates. The key class of enzymes for callose synthesis is the Callose Synthases. The callose synthase genes (*calS*) expression is modulated for biotic and abiotic stresses. In this study, nine *C. sinensis calS* genes (*Cscals*) were identified and the expression patterns were analyzed in *CaLas* inoculated and healthy plants. At 120 days after inoculation (dpi), *Cscals2* and *Cscals7* were significantly up-regulated in the HLB positive plants. At 360 dpi *Cscals7* and *Cscals12* were significantly up-regulated in the HLB positive plants. Our results confirmed that *CaLas* infection is accompanied by the increased deposition of callose in the phloem sieve tubes and accumulation of starch in the leaves. It is suggested that the increased deposition of callose in the phloem sieve tubes is a hypersensitivity reaction, inhibiting phloem transport to consequently reducing

the bacterial colonization via phloem, what possibly contribute to the starch accumulation in the leaves and the development of HLB symptoms. It is also proposed that *Cscals2*, *Cscals7* and *Cscals12* are involved in citrus defense against *CaLas*, forming a complex in the phloem.

**Keywords** Callose · Phloem · Citrus · HLB · Defense

## Introduction

Plants response against pathogens by induction of several biochemical mechanisms like activation of signaling pathways, production of reactive oxygen species (ROS) or physiological changes such as the thickening of the cell walls responses by callose deposition (Jones and Dangl 2006).

Callose is a polymer of  $\beta$ -1,3-glucan units (Chen and Kim 2009), which is present under normal conditions on cell walls, root hair, spiral thickenings in tracheids, pollen grains, pollen tubes (Chen and Kim 2009; Stone and Clarke 1992) and plays important role in intercellular water transport, cell growth and differentiation (Nedukha 2015). Furthermore, it has been localized on phloem sieve plates and at the cell plasmodesmata to regulate the cell-to-cell movement of molecules by controlling the size exclusion limit (Ellinger and Voigt 2014). However, under stress conditions, including wounding, pathogen infection or physiological stress, callose accumulates rapidly and drastically, blocking the sieve plates, reducing the functionality of

**Electronic supplementary material** The online version of this article (<https://doi.org/10.1007/s10658-019-01747-6>) contains supplementary material, which is available to authorized users.

L. M. Granato (✉) · D. M. Galdeano ·  
N. D. R. D'Alessandre · M. C. Breton · M. A. Machado  
Centro de Citricultura Sylvio Moreira/IAC, Rodovia Anhanguera  
Km. Cordeirópolis, SP 158, Brazil  
e-mail: laisgranato@gmail.com

the phloem, interfering with the transport of carbohydrates from the source organs (mainly leaves) to the sink organs (roots, flowers, fruits) (Nishimura 2008).

The key class of enzyme for callose synthesis is Callose Synthase (CaS) (Richmond and Somerville 2000), also referred to as glucan synthase-like (GLS), which contains multiple transmembrane segments and a hydrophilic central loop (Verma and Hong 2011). Callose is synthesized in several locations in plants (Stone and Clarke 1992), and CaS responds to developmental and environmental signals, including biotic and abiotic stresses, it is conceivable that different isoforms of CaS may constitute different complexes at each site.

In *Arabidopsis thaliana* 12 callose synthase (*AtCaS*) genes were identified and characterized (Richmond and Somerville 2000). Among them, *AtCaS7* has been associated with the synthesis of callose in the sieve plate of phloem in response to stresses (Xie and Hong 2011). The evaluation of *A. thaliana calS7* mutants demonstrated the malformation of the pores in the sieve plate with narrowing or blockage of (Xie et al. 2011). In these conditions, the phloem became non-functional and there was accumulation of starch in the leaves (Barratt et al. 2011). In addition, others *AtCaS* have already been reported by the involvement with plant defense response against pathogen infection, including *AtCaS2*, *AtCaS5*, *AtCaS8* and *AtCaS12*. The expression of *AtCaS2*, *AtCaS5* and *AtCaS8* genes were induced in *Arabidopsis* rosette leaves after salicylic acid (SA) treatment and *Hyaloperonospora arabidopsis* infection, playing a role in callose accumulation at plasmodesmal channels as a strategy to alter plasmodesmal permeability under pathogen infection (Cui and Lee 2016; Dong et al. 2008).

One of the most devastating diseases of citrus is Huanglongbing (HLB) (Bové 2006; Kim et al. 2009), whose symptoms include blotchy chlorosis and mottling of leaves, yellow shoot, vein corking, stunted growth, suppression of new root growth, and production of unmarketable fruits that are small, green, and lopsided, with aborted seeds (Bové 2006). These symptoms have been related to the high rate deposition of callose in the sieve plates pores of the phloem (Albrecht and Bowman 2008; Boava et al. 2017), induced by presence of the intracellular bacterium *Candidatus Liberibacter asiaticus* (*CaLas*), which is naturally transmitted by the psyllid *Diaphorina citri* (Bové 2006; Coletta-Filho et al. 2004).

Callose is an important mechanism of defense against invasive tissue pathogens, because it is a general mechanism of cell wall strengthening or blocking of sieve plates or plasmodesmata cells (Koh et al. 2012). However, the role of callose against intracellular pathogens inoculated by vectors, as HLB, is not fully known. For this, to decipher the mechanisms of callose synthesis in sweet orange phloem and its relationship with *CaLas* infection, we identified genes of the *Citrus sinensis* calloses synthases and analyzed their expression profiles that might be related to callose synthesis in sweet orange phloem during infection of *Ca. L. asiaticus*. Besides that, we evaluated callose deposition in the phloem sieve tubes and the starch buildup in the leaves.

## Material and methods

### Identification of CaS sequences

The CaS family genes of *Citrus sinensis* were identified using BLASTP queries of *Arabidopsis thaliana* genome (<https://www.arabidopsis.org>). The sequences of different CaS family genes from *Citrus sinensis* (<https://phytozome.jgi.doe.gov>) genome database. Synteny analyses between *C. sinensis* and *A. thaliana calS* sequences were performed using the percentage of identity by BLASTN (<https://blast.ncbi.nlm.nih.gov/>). The circular genomic region variation maps of *calS* were construct in the Circos software ([www.circos.ca](http://www.circos.ca)). The multiple sequence alignment was performed using Clustal Omega (Sievers et al. 2011) and the phylogenetic tree was constructed using the neighbor-joining method and MEGA7 (Kumar et al., 2016); bootstrap values were calculated from 1000 trees.

Evaluation of the distribution of the CaS genes in the *C. sinensis* and *A. thaliana* genomes was carried out by a genome architecture analysis, which was built based on a two-dimensional method of binary data using the R software. This method combines genome architecture heatmaps with scatter plots of the genomic environment and the pool of selected genes (Raffaële et al. 2010).

### Characterization of *C. sinensis* CaS sequences

The genomic coordinates of each *calS* gene from *C. sinensis* were used to determine their distribution in

the chromosomes. The coordinates were retrieved accessing the genome browser from each Citrus database.

The similarity of citrus callose synthases amino acid sequences was performed using BLASTP and taking the CalS7 sequence as reference. The bit score results obtained from the alignments with fixed  $E < 10^{-10}$  were visualized by the tool Circoletto (<http://tools.bat.infspire.org/circoletto/>). Conserved domains from each CalS proteins were predicted using NCBI's Conserved Domain Database and SMART (<http://smart.embl-heidelberg.de/>). To obtain the conserved regions, the multiple protein sequences alignment was generated using Clustal Omega (Sievers et al. 2011).

#### Plant material and treatments

Pera sweet orange (*C. sinensis* L. Osb.) was propagated using buds that were grafted onto rootstocks of a 6-month-old Rangpur lime (*C. limonia* Osb.). After 6 months, plants were graft inoculated with two *CaLas* infected budwoods, which were grafted on the opposite side of the plant's primary stem. Infected budwoods were left on the plants but shoots from these budwoods were eliminated upon sprouting. All plants were maintained in a greenhouse with an average temperature of 25°C. Five biological replicates for mock-inoculated (healthy budwood) and ten biological replicates for *CaLas* inoculated (infected budwood) were evaluated.

#### DNA extraction and *CaLas* quantification

Leaves of similar age, position and at the same developmental stage were collected from four sides of the plant. Petioles from five leaves were pooled and 200 mg were lysed by grinding with two beads (3-mm diameter) in 2-mL microtubes at 30 Hz for 120 s in a TissueLyser II (Qiagen). DNA extraction was carried out using the CTAB method as described before (Murray and Thompson 1980). Precipitated DNA was dissolved in 40  $\mu$ L of DNase-free water and its quality was checked by electrophoresis in 1.0% agarose gels. DNA concentration was determined using a NanoDrop<sup>TM</sup> 8000 spectrophotometer (Thermo Scientific) and adjusted to 100 ng/ $\mu$ L. The degree of *CaLas* infection was quantified by qPCR using a standard curve with 10-fold serial dilutions of 16S ribosomal DNA (rDNA) cloning into pGEM@-T vector (Promega). The bacterial titer was evaluated according to Boava et al. 2015.

#### RNA extraction and cDNA synthesis

Total RNA was using CTAB method (Murray and Thompson 1980) and to RNA precipitation was used Lithium chloride (LiCl) protocol. Genomic DNA was eliminated using DNase (Thermo Scientific). RNA quality was verified by ethidium bromide staining after separation on 1.0% agarose gel. RNA concentration was determined using a NanoDrop ND-8000 spectrophotometer (Thermo Scientific). cDNA was synthesized from 1.0  $\mu$ g of total RNA using iScript cDNA Synthesis kit (Bio-Rad) according to the manufacturer's instructions.

#### Analysis of *calS* expression by quantitative real-time PCR (qPCR)

Expression of *C. sinensis* CalS genes were evaluated in the early stages of infection at one and 7 days post inoculation (dpi), and in the late stages of infection at 120 and 360 dpi.

Primers were designed using Primer Blast software (<https://www.ncbi.nlm.nih.gov/tools/primer-blast/>) and checked by the Gene runner tool (Table 1). Amplicon lengths ranged between 100 and 120 bp and annealing temperature of 60°C. Amplicons were sequenced on the ABI 3730 sequencer (Applied Biosystems, Foster City, CA, USA) using DyeTerminator chemistry.

PCR primer efficiency of each primer pair was also determined using the Real-time PCR Miner (<http://ewindup.info/miner/>). RT-qPCR was performed using the GoTaq qPCR Master Mix (Promega). The reaction mixture consisted of 3.0  $\mu$ L cDNA and 120 nM of each gene-specific primer in a final volume of 12  $\mu$ L. Amplification was carried on three replicates of each sample with appropriate negative controls on an ABI PRISM 7500 SDS (Applied Biosystems) thermal cycler with the following conditions: 50°C for 2 min, 95°C for 10 min; 40 cycles of 95°C for 15 s, and 60°C for 1 min.

The gene expression levels were quantified based on the number of amplification cycles needed to reach a common fixed threshold (cycle threshold – Ct) in the exponential phase of the PCR. For relative quantification, the  $2^{-\Delta\Delta CT}$  method was applied (Livak and Schmittgen 2001). Gene expression was showed as fold change in *CaLas* infected samples compared to the respective healthy plant (mock) with GAPDH and EF1K as reference genes (Mafra et al. 2012).

**Table 1** Primers pairs used for amplification of calose synthase genes of sweet orange

Primers	Sequences (5'- 3')	Reference
<i>Cscals2</i>	F, ATCTCTGCCGGTTCTATGCG R, CGGGCATCACTCTT TGACCT	This study
<i>Cscals3</i>	F, GGCCTCCGTTCTTACTTGCT R, ACACTCCTTGACAG CACAGG	This study
<i>Cscals5</i>	F, GTGTGATTGAAACG GAAGCCA R, CCATCATCACGCAT AGGCCA	This study
<i>Cscals7</i>	F, GACGCCTAACCGAG TACCTGC R, GTGCAGCTGGTGAT CCATCA	This study
<i>Cscals8</i>	F, AGGATGTTTTTCGCC GGTACA R, ATCACGACCTTTGC CCACTT	This study
<i>Cscals9</i>	F, TCCTTTCTCGAATTGGCCGT R, TGCTGTGCGCGAT ATGAGG	This study
<i>Cscals10</i>	F, GGCTCGACTTGGCA TACCTG R, AACTGTTCCAAGCA AGGCGT	This study
<i>Cscals11</i>	F, GATGTGTACCGCTT GGGTCA R, AGCAAGATAAAGAC GCCCCC	This study
<i>Cscals12</i>	F, CTTGGGTCAGCGTG TTTTGG R, CTCCTCGCAGTG CAGTTA	This study
GAPDH	F, GGAAGGTCAAGATC GGAATCAA R, CGTCCCTCTGCAAG ATGACTCT	(Mafra et al. 2012)
EF1- $\alpha$	F, TCAGGCAAGGAGCT TGAGAAG R, GGCTTGGTGGGAAT CATCTTAA	(Mafra et al. 2012)

### Callose analysis

Total callose was observed by microscopy analysis of petioles of leaves. The petiole from both inoculated and mock-inoculated plants from 30, 120 and 360 dpi were immediately transferred to the FAA solution (50 mL of 37% formaldehyde, 50 mL glacial acetic acid and

900 mL of 70% ethanol) (Koh et al. 2012). After 72 h incubation in FAA solution, the samples were maintained in 70% ethanol. The samples were incubated for 30 min in 0.15 M phosphate buffer (pH 9.5) containing 0.01% aniline blue (Jin and Mackey 2017). The stained samples were examined on an Olympus BX61 fluorescent microscope using 355–375 nm excitation filter, 400-nm dichromatic mirror, and 435–490 nm emission filter. Five leaf samples from each plant and ten longitudinal sections from each sample were examined. Callose deposition was quantified by measurement of the relative fluorescence intensity emitted by aniline blue stain using ImageJ (Version 1.45 s) (<https://imagej.nih.gov/ij/>).

### Starch quantification

To quantify total starch, leaves were collected at 30, 60, 120, 180, 240 and 360 days after inoculation. The leaves were dried in an oven at 60°C for 48 h. The dried material was ground using two beads (3-mm diameter) in 2-mL microtubes at 30 Hz for 120 s on a TissueLyser II (Qiagen) and subjected to starch quantitation. Starch content was estimated by enzymatic analysis using 10 mg of dried leaves according to Amaral et al. (2007). Absorbance was measured in a 96-well microtiter plates using a Microplate Reader (Model 3550 – BIO-RAD) at 490 nm. A standard curve was performed using a glucose solution (SIGMA) at concentrations of 0; 2.5; 5.0; 7.5 and 10  $\mu\text{g mL}^{-1}$ .

### Statistical analysis

Student's t test was used to calculate significant differences. Spearman's rank correlation coefficient value was estimated using the Minitab® Statistical Software (<http://www.minitab.com>). An association between gene expression, callose deposition and starch accumulation was tested by considering *P* value (threshold = 0.05).

### Results

Identification of *Citrus sinensis* CalS sequences, phylogenetic analysis and genome architecture

Callose synthase sequences of *A. thaliana* were used in BLASTX queries against the *C. sinensis* genome

sequences. Nine putative callose synthase (CalS) genes were identified, and named according to the CalS as *Cscals2*, *Cscals3*, *Cscals5*, *Cscals7*, *Cscals8*, *Cscals9*, *Cscals10*, *Cscals11* and *Cscals12* based on their sequence similarity to *AtcalS* (Verma and Hong 2011). Polymorphism associates to *CsCalS* and *AtCalS* gene sequences were visualized in the “CIRCOS” software (Fig. 1). Sequence similarity among the *CsCalS* and *AtCalS* proteins, predicted by BLASTP, varied from 41 to 83% (Fig. 1a). However, the sequences predicted by BLASTN changed from 0 to 80% allowing identification of the *Cscals* sequences corresponding to *AtcalS* (Fig. 1b). Thus, *AtcalS9* and *Cscals9*, and *AtcalS8* and *Cscals8* revealed 70% of identity among them, on the other hand, *Cscals7* is 76% similar to *AtcalS7* and *AtcalS6*.

Phylogenetic analysis among the *CsCalS* and *AtCalS* suggests that CalS families may be divided into three main groups (Fig. 2a). The first group is formed by *AtCalS9*, *CsCalS9*, *AtCalS10*, *CsCalS10*, *AtCalS11*, *CsCalS11*, *AtCalS12*, *CsCalS12*, *AtCalS5* and *CsCalS5*; the second group by *AtCalS8*, *CsCalS8*, *AtCalS1*, *AtCalS2*, *AtCalS4*, *CsCalS2*, *AtCalS3* and *CsCalS3*, and the third group is composed by *AtCalS6*, *AtCalS7* and *CsCalS7*.

The distribution of CalS gene in the genome of sweet orange is shown in the genome architecture (Fig. 2b). The

analysis was performed regarding the flanking intergenic distances (FIR) of CalS genes, pointing out a dense (lower size of intergenic regions) and sparse regions. The gene distribution along the genome was continuous, suggesting that most genes have a medium to large intergenic region size, which allows that many evolution changes can occur over time. Most callose synthase genes are in medium and large intergenic regions in *C. sinensis* architecture (third and fourth quadrants).

### Characterization of *CsCalS*

*Cscals2* and *Cscals7* were located in chromosome 7; *Cscals8* and *Cscals10* were located in chromosome 5; *Cscals5* and *Cscals11* were located in chromosomes 1 and 2, respectively. However, the *Cscals9* and *Cscals12* were located in chromosome unknown (Table 2). The *CsCalS* transcript sequences ranged from 5800 to 7912 bp (Table 2), encoding 1771 to 1978 amino acid.

The identity among *CsCalS* sequences predicted by BLASTX ranged from 42 to 82% (Fig. 3). For example, *CsCalS7* share 57% and 44% of identity with *CsCalS3* and *CsCalS12*, respectively (Table 3). Moreover, the *CsCalS* amino acid sequences shown high homology in the domain region (Supplementary Fig. 1). However,

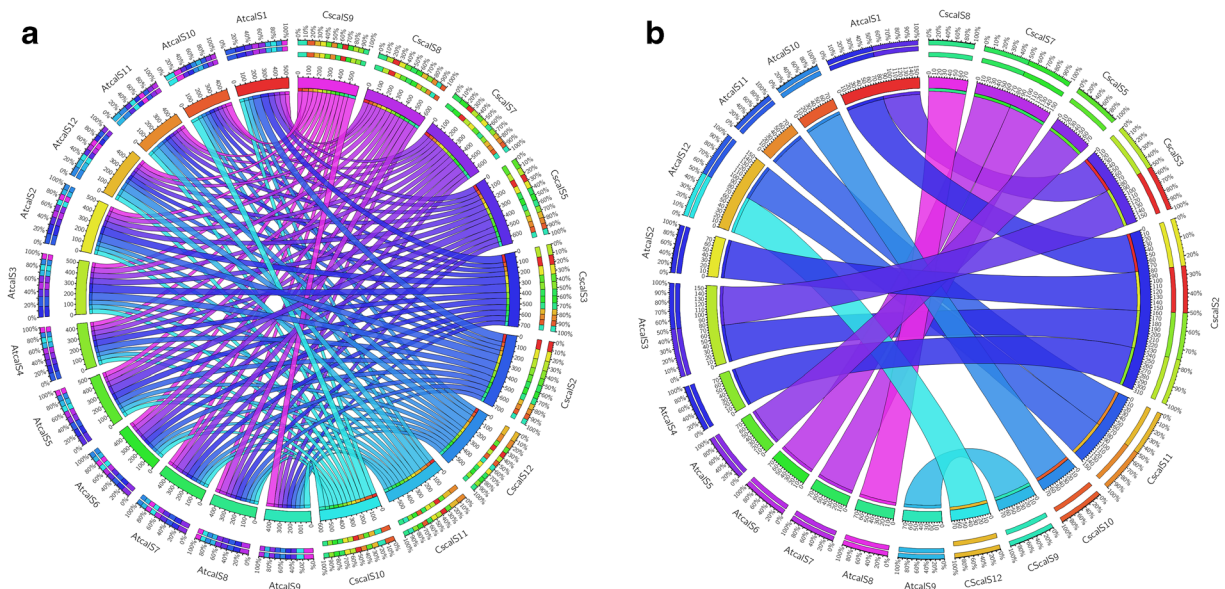


**Fig. 1** Polymorphism of callose synthase sequences from *C. sinensis* (*Cscals*) and *A. thaliana* (*AtcalS*). **a** Similarity predicted by BLASTP among the sequences of *Cscals* (on the right) and *AtcalS* (on the left). **b** Similarity predicted by BLASTN

among the sequences of *Cscals* (on the right) and *AtcalS* (on the left). Each color represents one CalS sequence, and the wider the ribbons represents the larger the percentage of identity among the sequences

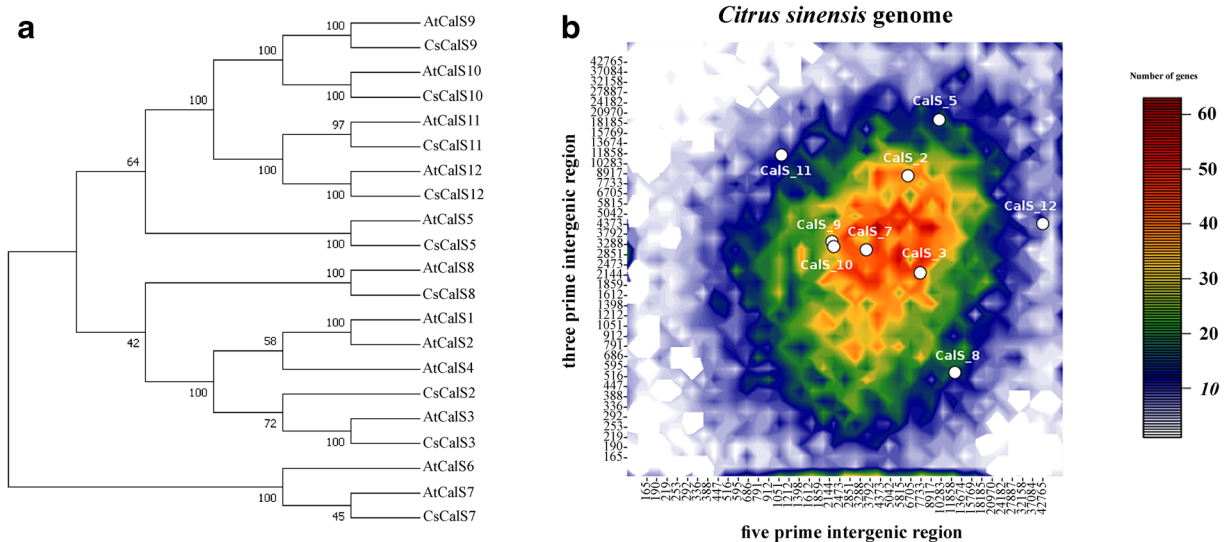


**Fig. 2** Sequence analysis of callose synthase. **a** Phylogenetic analysis of *C. sinensis* and *A. thaliana* CalS proteins using MEGA neighbor-joining. Numbers at the branch points are bootstraps values. *CsCalS*: *C. sinensis* CalS proteins; *AtCalS*: *A. thaliana* CalS proteins. *AtCalS1* (AF237733.1), *AtCalS2* (NM\_179847.1), *AtCalS3* (NM\_121303.6), *AtCalS4* (NM\_123045.2), *AtCalS5*

(NM\_179622.2), *AtCalS6* (NM\_115772.2), *AtCalS7* (NM\_100528.1), *AtCalS8* (NM\_112317.1), *AtCalS9* (NM\_111596.5), *AtCalS10* (GQ373182.1), *AtCalS11* (NM\_116736.1), and *AtCalS12* (NM\_116593.3). **b** Position of CalS on the flanking intergenic regions (FIR) *C. sinensis* heat map

the C-terminal regions sequences of *CsCalS* showed low homology in silico analyzes, what was confirmed by the DNA sequencing.

One FKS1 domain, one b-1,3-glucan synthase domain and several transmembrane domains (Fig. 4) which were conserved among CalS families were identified in *CsCalS*. The FKS1 domain encode alternative catalytic

subunits of the glucan synthases that are responsible for synthesis of beta-1,3-glucan, it is likely to be the ‘Class I’ region just N-terminal to the first set of transmembrane helices. The number of transmembrane domains situated at N-terminal are more variable than at C-terminal. *CsCalS7* has four N-terminal transmembrane domains, *CsCalS2*, *CsCalS11* and *CsCalS12* have two N-terminal transmembrane domains, while *CsCalS3*, *CsCalS5*, *CsCalS8*, *CsCalS9* and *CsCalS10* have just one N-terminal transmembrane domain (Fig. 4).

**Table 2** Chromosome location of CalS genes in *Citrus sinensis* (sweet orange)

Gene <sup>a</sup>	Acession number	Chromosome location	CDS (bp)
<i>Cscals2</i>	LOC102624514	chr7:117645.130605	6472
<i>Cscals3</i>	LOC102611841	chrUn	6301
<i>Cscals5</i>	LOC102618167	chr1:5590391.5608446	6271
<i>Cscals7</i>	LOC102612996	chr7:12958535.12980191	6411
<i>Cscals8</i>	LOC102631245	chr5:12747408.12763544	6392
<i>Cscals9</i>	LOC102612131	chrUn	6089
<i>Cscals10</i>	LOC102616583	chr5: 4180303.42122762	6359
<i>Cscals11</i>	LOC102627313	chr2:3385239.3391324	7912
<i>Cscals12</i>	LOC102610237	chrUn	5800

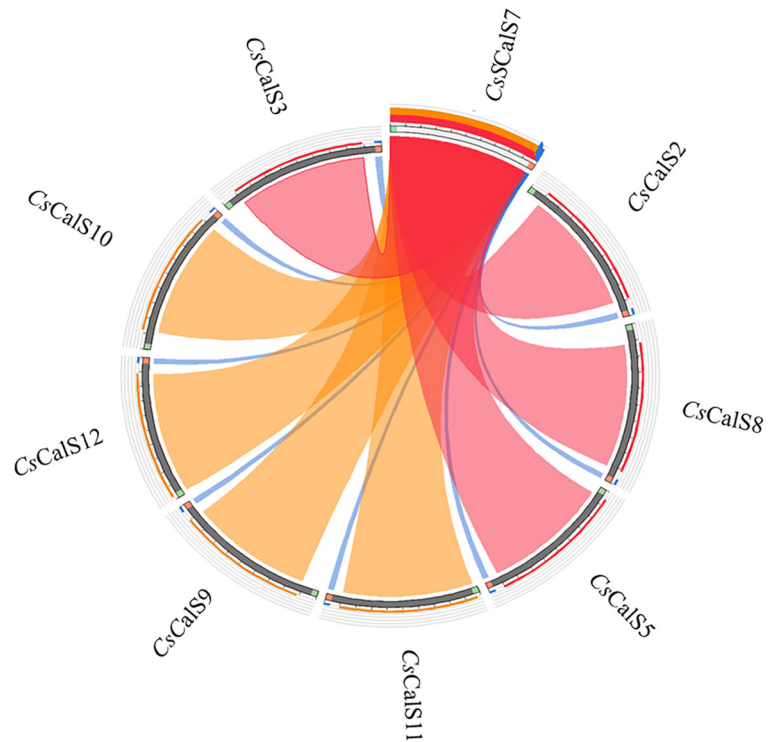
<sup>a</sup>The number to each *Cscals* gene was assigned on the basis of homology with *AtcalS*

Un Unknown chromosome

#### Expression of *CsCalS* genes in response to *CaLas*

Expression profile of *CsCalS* genes in response to *CaLas* infection were analyzed in both plants inoculated with healthy budwood (healthy plants) and plants inoculated with *CaLas* infected budwood (HLB+), which were confirmed by PCR (Supplementary Fig. 2). The expression of *CsCalS* genes were evaluated at 120 and 360 dpi. *CsCalS* genes expression was also evaluated at 1 and 7 dpi (early stages), but no significant differences were observed between HLB positive and healthy plants (data not shown). *CsCalS2* and *CsCalS7* were significantly up-regulated in the HLB positive plants at 120 dpi. At 360 dpi the *CsCalS7* and *CsCalS12* were significantly up-regulated in the HLB positive plants (Fig. 5).

**Fig. 3** Identity visualization of the amino acid sequence of *CsCalS*. *CsCaS7* was used as a query against the other *CsCalS*. The red color represents sequences that are more similar (bitscores >80%) than those that are in orange



Callose deposition and starch accumulation is positive correlated with *Cscals* gene expression

Microscopy analysis was performed to evaluate callose accumulation into the phloem sieve tubes after infection with *CaLas*. Callose deposition was observed in both healthy and infected phloem sieve tubes. However, callose accumulation in the HLB positive phloem sieve tubes are more abundant when compared to healthy phloem sieve tubes, and higher at 360 dpi than at 120

dpi. At 360 dpi the difference of the callose content between HLB positive and healthy plants was significant ( $P < 0.05$ ). Despite the great difference of callose deposits between plants, the callose deposits in the phloem cells of the HLB positive petioles were about two times higher than healthy phloem cells, either at 120 dpi as at 360 dpi (Fig. 6).

Starch content was estimated by enzymatic analysis to investigate changes in its abundance during infection in leaves of all plants used in this study. After 60 dai,

**Table 3** Percentage (%) of the identity among *CsCalS* sequences predicted by BLASTX

	<i>CsCalS2</i>	<i>CsCalS3</i>	<i>CsCalS5</i>	<i>CsCalS7</i>	<i>CsCalS8</i>	<i>CsCalS9</i>	<i>CsCalS10</i>	<i>CsCalS11</i>	<i>CsCalS12</i>
<i>CsCalS2</i>	100	82	60	56	56	45	45	45	45
<i>CsCalS3</i>	82	100	61	57	57	45	46	47	47
<i>CsCalS5</i>	61	63	100	54	54	46	47	49	47
<i>CsCalS7</i>	55	55	54	100	52	45	45	44	44
<i>CsCalS8</i>	55	56	52	52	100	42	42	45	44
<i>CsCalS9</i>	44	45	51	46	42	100	65	44	45
<i>CsCalS10</i>	45	46	47	46	42	65	100	45	46
<i>CsCalS11</i>	45	47	47	44	45	44	45	100	74
<i>CsCalS12</i>	45	47	46	44	44	45	46	46	100

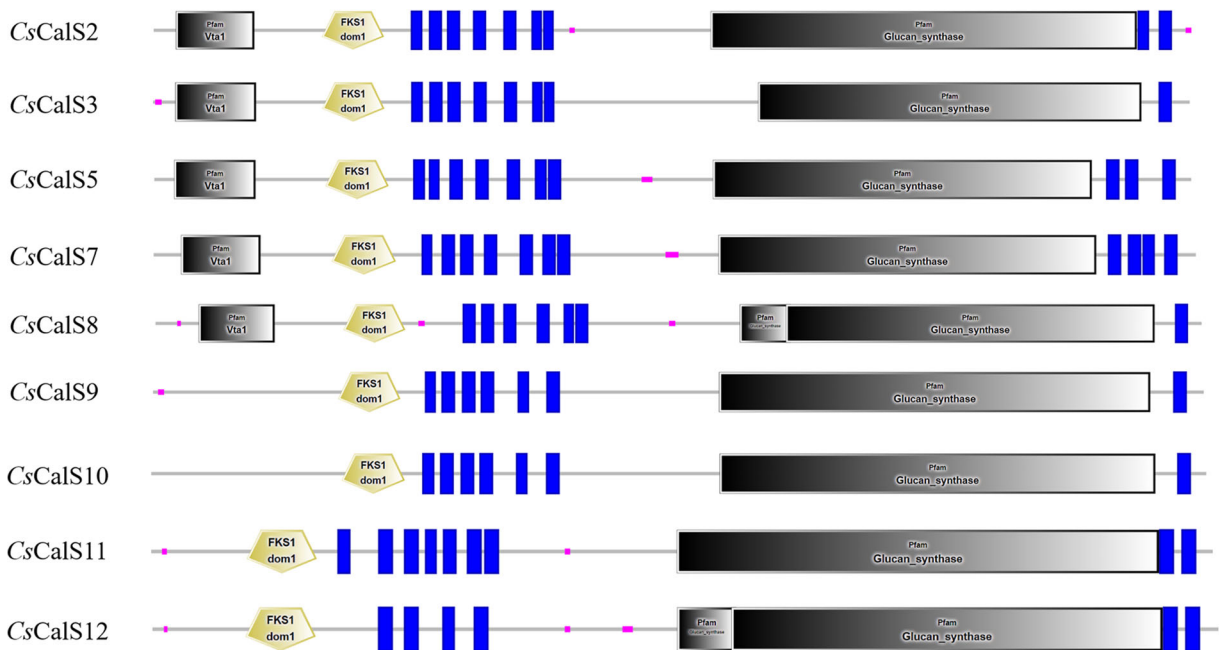


**Fig. 4** Domain structure of *CsCalS* proteins. The deduced amino acid sequences of *Citrus sinensis calS* genes were analyzed using the SMART tool (<http://smart.embl-heidelberg.de/>). FKS1 domains were indicated by yellow pentagon, transmembrane

domains were in vertical blue bars and glucan synthase domains were in long gray rectangle. Domains with scores less significant than established cutoffs are not shown in the diagram

starch amount in HLB positive leaves were significantly higher than leaves obtained from plants inoculated with healthy budwood (Fig. 7). At 120 dpi, the starch amount reached the highest relative value in compare the other times evaluated. At 180 dpi, the starch content was seven-fold higher in HLB positive leaves compared with healthy leaves. The difference between HLB positive and healthy leaves was three and two-fold higher at 240 and 360 dpi, respectively (Fig. 7).

The plants were tested for a correlation between callose deposits, starch content and gene expression. The correlation coefficient revealed that callose deposits has a positive correlation with the starch content either at 120 dpi (0.943,  $P < 0.05$ ) as 360 dpi (0.810,  $P < 0.05$ ) (Table 4). At both evaluated times, *CscalS7* was the only gene which showed a positive correlation with callose deposition and starch content, although the coefficient values are not significant.

## Discussion

By comparing the sequence of *A. thaliana* callose synthase genes, nine *CsCalS* genes were identified in the *C. sinensis* genome (Fig. 1; Fig. 2a). The *CsCalS* genes

were found in the sparse region of the *C. sinensis* genome, showing genome regions with large flanking intergenic regions (FIR) either in the three prime as in the five prime regions (Fig. 2b). FIR have high density of active regulatory elements (Sinzelle et al. 2009), which can be more susceptible to translocations, deletions, duplications, insertions and point mutations (Scacheri and Scacheri 2015). This characteristic turn the FIR plastic and responsible for adaptability (Raffaele et al. 2010). It is suggested that callose synthases of *C. sinensis* can be susceptible to evolution changes due to the existing selection pressure, such as abiotic and biotic stresses.

Aminoacid sequences analyzes showed high similarity among the *CsCalS* (Fig. 3). Despite the high similarity, the DNA sequencing of the corresponding C-terminal protein regions allowed the differentiation of the *CsCalS* genes (data not shown). All *CsCalS* seem to be membrane proteins, with six to 12 transmembrane domains (Fig. 4). The predicted function of Calloses Synthases is based on their homology with the FKS1 (FK506 SENSITIVITY) genes, which encode subunits of 1,3-beta-glucan synthase complexes in *Saccharomyces cerevisiae* (Douglas et al. 1994). *S. cerevisiae* FKS1 sequence consists of two large hydrophobic domains,



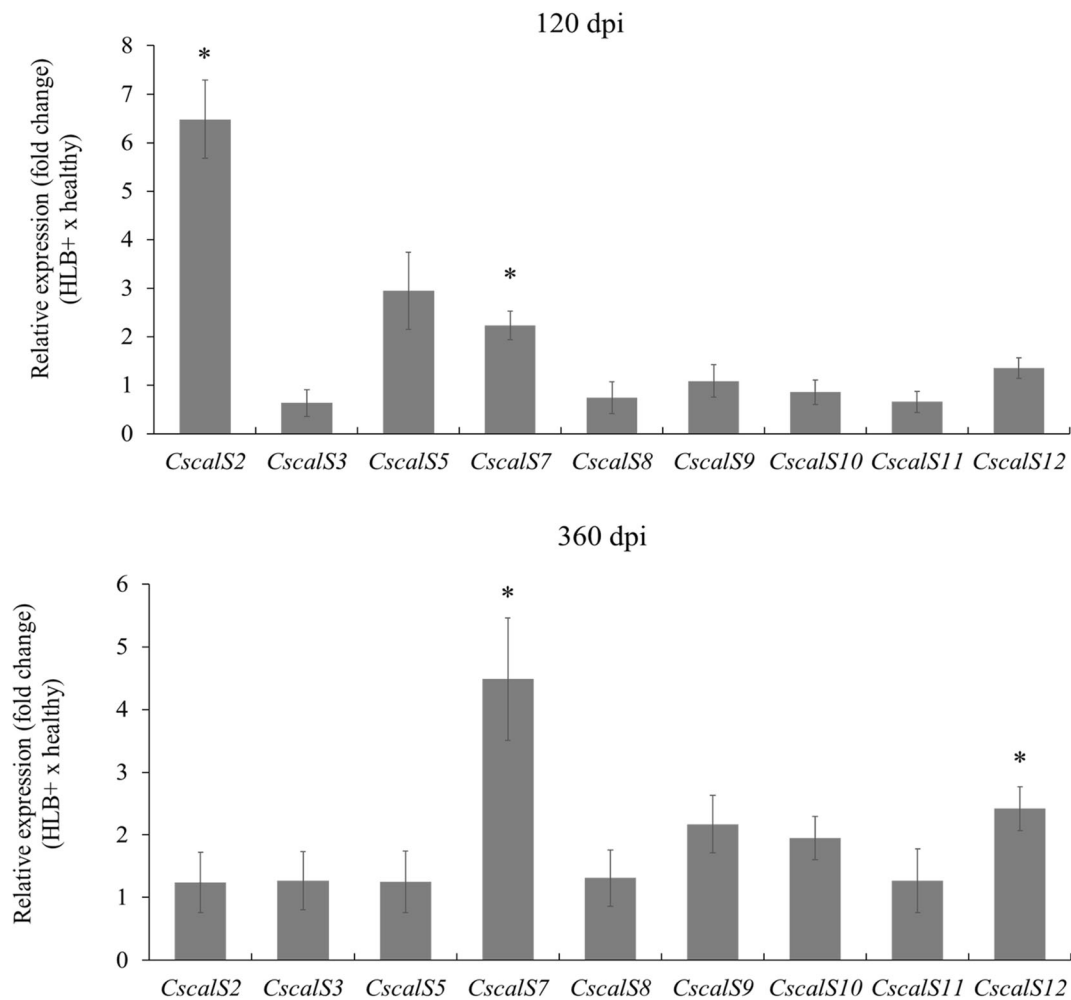


**Fig. 5** Comparison of *CsCalS* gene expression in leaves of sweet orange plants inoculated with health budwood (health plants) and inoculated with *CaLas* infected budwood (HLB+). The data are presented as fold change of health plants (five biological

replicates) compared to the expression of HLB+ plants (ten biological replicates). GAPDH and EF1K were used as reference genes. \* indicate significantly different *p*-values ( $P < 0.05$ ) in Student's *t* test

with several transmembrane helices, preceded by large cytoplasmic hydrophilic domains, that are characteristics from plasma membrane proteins (van Geest and Lolkema 2000). Plant CalS and fungal FKS homologues have been classified into a new glycosyltransferase superfamily, enzymes that catalyze the transfer of sugar monomers from activated donor molecules to specific acceptor molecules, forming glycosidic bonds (Lairson et al. 2008). The 1,3-beta-glucan synthase is an UDP-glycosyltransferase (UGT), which uses UDP-glucose in the transfer reaction (Li et al. 2001).

CalS genes are evolved in higher plants for the synthesis of callose in different tissues and in response to different physiological and developmental signals

(Verma and Hong 2011). Ellinger and Voigt (2014) reported that the expression of *AtCalS* genes are regulated in a tissue-specific manner. Nevertheless, in this work we showed that all *CsCalS* were expressed at *C. sinensis* leaves, which indicates that multiple *CsCalS* genes can be expressed in the leaves, as well as was demonstrated previously to *Arabidopsis* (Dong et al. 2008). The expression of *CsCalS* genes was evaluated at 120 and 360 days after inoculation of *CaLas*. At 120 dpi, the *Cscals2* and *Cscals7* were significantly up-regulated in the HLB positive plants (Fig. 5a), and at 360 dpi the *Cscals7* and *Cscals12* were significantly up-regulated in the HLB positive plants (Fig. 5b). It is known that many biotic and abiotic factors may affect

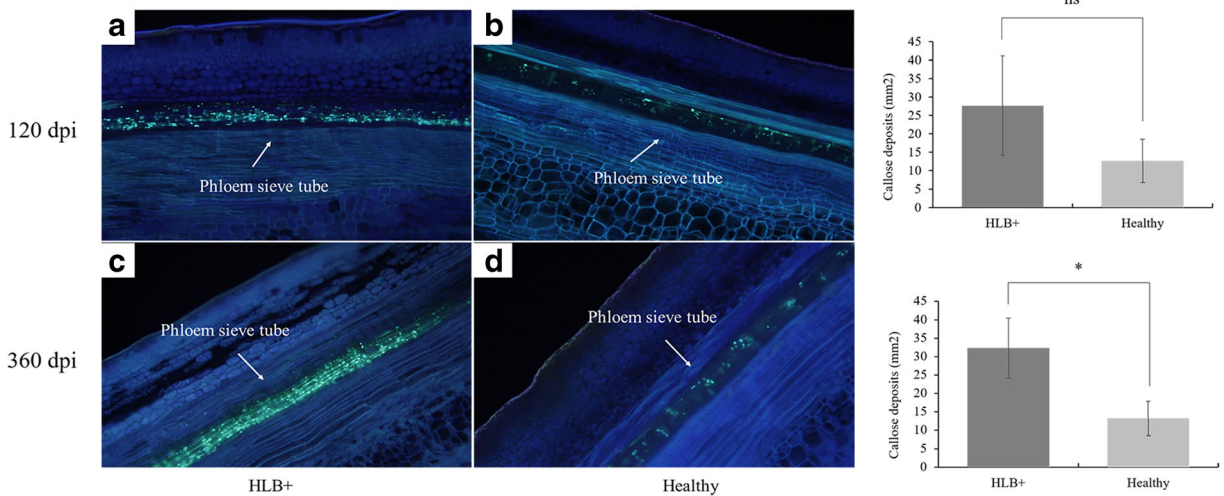


**Fig. 6** Callose deposition into the phloem sieve tubes of sweet orange HLB positive (**a** and **c**), and healthy (**b** and **d**) plants (10x). \*Indicates significant difference ( $P < 0.05$ ) and ns indicates no significance

the CalS activity in plants. For instance, in *A. thaliana*, *AtCalS1*, *AtCalS5*, *AtCalS9*, *AtCalS10*, and *AtCalS12* play role in defense response to pathogen infection (Dong et al. 2008; Jacobs 2003). Besides that, *AtCalS3*, *AtCalS7*, and *AtCalS11* play key roles in plant growth and reproduction (Enns et al. 2005; Xie et al. 2011). In grapevine cultivars, *Muscadina rotundifolia* ‘Noble’ and ‘Carlos’, *Vitis amurensis* ‘Shuanghong’ and

‘Zuoshanyi’, and *Vitis vinifera* ‘Chardonnay’, the genes *calS1*, *calS3*, *calS7*, *calS8*, *calS9*, *calS10*, and *calS11* were all up-regulated after *Plasmopara viticola* infection, suggesting that these CalS genes may be involved in defense responses against this mildew (Yu et al. 2015).

Both the *AtcalS1* and the *AtcalS2* had induced expression in *Arabidopsis* rosette leaves after salicylic acid

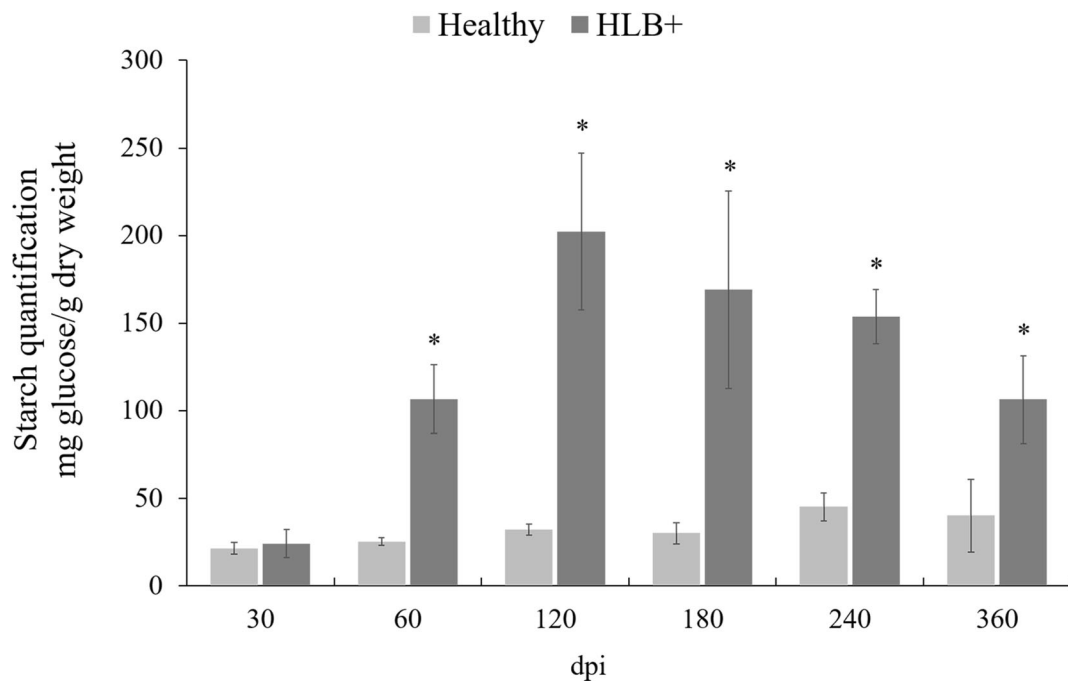


**Fig. 7** Temporal quantification of starch from sweet orange leaves after *CaLas* inoculation. \* indicate significantly different  $p$ -values ( $P < 0.05$ ) in Student's  $t$  test

**Table 4** Spearman's rank correlation coefficients among callose deposits, starch content and gene expression levels. \* Significant at  $P < 0.05$ 

	120 dpi		360 dpi	
	Callose	Starch	Callose	Starch
Starch	0.943*		0.810*	
CsCalS2	0.200	0.400	-0.286	-0.214
CsCalS3	-0.600	-0.700	-0.250	-0.300
CsCalS5	-0.400	-0.200	-0.317	-0.267
CsCalS7	0.400	0.400	0.381	0.167
CsCalS8	-0.500	-1.000	-0.200	-0.250
CsCalS9	-0.800	-0.600	-0.017	-0.150
CsCalS10	0.400	0.000	-0.119	0.000
CsCalS11	-0.100	-0.400	-0.200	-0.233
CsCalS12	-0.800	-0.600	0.238	0.452

(SA) treatment and *Hyaloperonospora arabidopsis* infection (Cui and Lee 2016; Dong et al. 2008). *AtCalS2* shares very high homology (92% identity) with *AtCalS1*, which suggests that a gene duplication event may have occurred (Hong et al. 2001). In this study, we showed the *CsCalS2* similarity with *AtCalS1*, *AtCalS2*, *AtCalS3* and *AtCalS4* (Fig. 1b), belonging to the same phylogenetic group (Fig. 2a). Due the high similarity, it is possible that *CalS1* and *CalS2* genes are functionally redundant (Hong et al. 2001). *CalS2* possibility plays a role in callose accumulation at plasmodesmal channels as a strategy to alter plasmodesmal permeability under pathogen infection, as it has been demonstrated for *CalS1* (Cui and Lee 2016; Dong et al. 2008). Moreover, the biological role of *CalS12* in plants was well studied in stress and pathogen response. This gene was induced by SA treatment (Dong et al. 2008), and is required for the deposition of callose in the cell wall thickenings at sites of fungal pathogen attack during powdery mildew infection (Ellinger and Voigt 2014; Nishimura 2008; Yu et al. 2015). Furthermore, callose deposition induced by *flg22*, an elicitor derived from the flagellin of bacterial pathogens (Gómez-Gómez et al. 1999; Zou et al. 2012), was entirely dependent on *CalS12* activity (Luna et al. 2011).

*CsCalS7* gene was the only gene differentially expressed in both evaluated times after *CaLas* infection (120 and 360 dpi). *AtCalS7* has been responsible for deposition in phloem sieve plates (Barratt et al. 2011;

Xie and Hong 2011). For instance, *calS7* mutant plants failed to synthesize callose in the plasmodesmal pores at the beginning of the pore construction, which leads to the formation of narrow or blocked sieve pores (Xie and Hong 2011) and reduce the transport of phloem sap. It has also been observed that the *CalS7* gene was remarkably up-regulated after 6 and 12 h of *P. viticola* infection in immune grapevine (*Muscadinia rotundifolia* 'Carlos') and resistant grapevine (*Vitis amurensis* 'Shuanghong'). Researchers have demonstrated the activation of defense pathway in citrus plants after *CaLas* infection for example, up-regulation of SA pathway genes, inducing callose accumulation and leading to clogging of phloem sieve pores (Aritua et al. 2013; Boava et al. 2017; Koh et al. 2012). Moreover, Dong et al. (2008) showed that *CalS* genes have induction of expression in response to SA. Thus, we suggest that the citrus defense response pathway may induce the up-regulation of *CsCalS7* against *CaLas* infection, which would be responsible for the deposition of callose at phloem sieve pores.

Phloem blockage has been suggested to be a major reason for HLB disease symptom development (Boava et al. 2017; Kim et al. 2009; Wang and Trivedi 2013; Zou et al. 2012), and this occur partially due to the deposits of large amounts of callose, as observed by previous reports (Kim et al. 2009). In our work, the staining with aniline blue confirmed the high deposition of callose in the phloem of HLB positive plants at 120 and 360 dpi (Fig. 6). It was suggested that the fully occupied sieve tubes at sink tissues might affect the integrity of the phloem and disrupt the osmotically generated pressure gradient that drives the phloem mass flow (Wang et al. 2017). The phloem blockage causes disturbance of photo-assimilate flows from source organs (leaves) to sink organs (roots) resulting in starch accumulation in the leaves chloroplast, as has been observed to HLB-affected trees (Etxeberria et al. 2009). In this study, the starch quantification of HLB positive leaves were significantly higher than leaves obtained from healthy plants after 60 dpi (Fig. 7) and reached the highest relative value at 120 dpi. It is believed that the excessive starch buildup cause breakdown of the chloroplast thylakoid system, producing the yellowing leaf mottle symptom, typical symptom of HLB (Bové 2006; Etxeberria et al. 2009). Therefore, the starch accumulation in leaves, appears to be a consequence of the reduction of transport of photo-assimilates to the sink organs.

We also showed the positive correlation between *CaLas* presence, callose deposits and starch content (Table 4), which are in agreement with previous studies that exhibited significant positive correlation between these three factors (Aritua et al. 2013; Boava et al. 2017; Etxeberria et al. 2009; Koh et al. 2012). Although not significant, *Cscals7* showed a positive correlation with callose deposition and starch content at both evaluated times, and also it has already been showed that loss of expression of *calS7* in *Arabidopsis* resulted in complete loss of the callose lining of sieve plate pores between phloem sieve elements (Xie et al. 2011; Xie and Hong 2011), what confirms the importance of this gene to callose deposition.

Alterations on gene expression can represent compatible or incompatible interaction between the host and pathogen (Jones and Dangl 2006; Kim et al. 2009). Incompatible interactions include the hypersensitivity response (HR) characterized by the programmed cell death at the infection site that restricts pathogen spread (Grant and Mansfield 1999). Therefore, callose accumulation and the consequent anatomical alterations of the sieve pores could be HR of the infected plants, whose main consequence would be isolate spatially the *CaLas* and reduce their colonizing ability via the phloem (Boava et al. 2017). The fact that no differences were found early after infection corroborate other authors who have demonstrated that defense associated genes have a very delayed expression after *CaLas* infection (Albrecht and Bowman 2008; Liao and Burns 2012).

In conclusion, our results suggested that sweet orange has nine calloses synthases and they are very similar to each other. The expression of *Cscals2*, *Cscals7* and *Cscals12* were up-regulated in HLB positive plants, suggesting these genes are affected in response to HLB to increase callose deposition. We assume that, probably, the increase of *Cscals* expression is a citrus defense response to rise callose deposition in the phloem, plugging the sieve pores to reduce the bacteria colonization. However, the blockage of sieve pores contributes to the accumulation of starch in the leaves and the development of HLB symptoms. For this reason, we believe that the gene silencing of *Cscals*, mainly of *Cscals7*, through genetic engineering could lead to decrease of callose in the *Citrus* phloem and consequently to reduction of HLB symptoms comparing with non-modified plants.

**Author's contributions** MAM and LMG conceived the project. LMG, MAM and NRD designed and performed the experiments. LMG, DMG and MCB analyzed the data. LMG, DMG and MAM wrote the paper. All authors read and approved the final manuscript.

**Compliance with ethical standards** This work has been supported by INCT Citrus (Proc. CNPQ 465440/2014–2 and FAPESP 2014/50880–0) and a CNPQ/PDJ fellowship (116424/2017–6). LMG and DMG are CNPQ post-doctoral fellows. NRD is a CNPQ undergraduate fellow. MAM is recipient of research fellowships from CNPq.

**Conflict of interest** The authors declare that they have no competing interests, inform consent and that this research did not involve human participants or animals.

**Open Access** This article is distributed under the terms of the Creative Commons Attribution 4.0 International License (<http://creativecommons.org/licenses/by/4.0/>), which permits unrestricted use, distribution, and reproduction in any medium, provided you give appropriate credit to the original author(s) and the source, provide a link to the Creative Commons license, and indicate if changes were made.

## References

- Albrecht, U., & Bowman, K. D. (2008). Gene expression in *Citrus sinensis* (L.) Osbeck following infection with the bacterial pathogen *Candidatus Liberibacter asiaticus* causing Huanglongbing in Florida. *Plant Science*, 175(3), 291–306. <https://doi.org/10.1016/j.plantsci.2008.05.001>.
- Amaral, L., Gaspar, M., Costa, P., Aidar, M., & Buckeridge, M. (2007). Novo método enzimático rápido e sensível de extração e dosagem de amido em materiais vegetais. *Hoehnea*, 34(4), 425–431. <https://doi.org/10.1590/S2236-89062007000400001>.
- Aritua, V., Achor, D., Gmitter, F. G., Albrigo, G., & Wang, N. (2013). Transcriptional and microscopic analyses of Citrus stem and root responses to *Candidatus Liberibacter asiaticus* infection. *PLoS One*, 8(9), 4–8. <https://doi.org/10.1371/journal.pone.0073742>.
- Barratt, D. H. P., Kölling, K., Graf, A., Pike, M., Calder, G., Findlay, K., et al. (2011). Callose synthase *GSL7* is necessary for normal phloem transport and inflorescence growth in *Arabidopsis*. *Plant Physiology*, 155(1), 328–341. <https://doi.org/10.1104/pp.110.166330>.
- Boava, L. P., Sagawa, C. H. D., Cristofani-Yaly, M., & Machado, M. A. (2015). Incidence of '*Candidatus Liberibacter asiaticus*'-infected plants among citrandarins as rootstock and scion under field conditions. *Phytopathology*, 105(4), 518–524. <https://doi.org/10.1094/PHYTO-08-14-0211-R>.
- Boava, L. P., Cristofani-Yaly, M., & Machado, M. (2017). Physiologic, anatomic, and gene expression changes in *Citrus sunki*, *Poncirus trifoliata* and their hybrids after

- Liberibacter asiaticus infection. *Phytopathology*, 107, 590–599. <https://doi.org/10.1094/PHYTO-02-16-0077-R>.
- Bové, J. M. (2006). Huanglongbing : A destructive , newly-emerging, century-old disease of Citrus. *Journal of Plant Pathology*, 88(1), 7–37. <https://doi.org/10.4454/jpp.v88.i1.828>.
- Chen, X., & Kim, J. (2009). Callose synthesis in higher plants. *Plant Signaling & Behavior*, 2324(August), 489–492. <https://doi.org/10.4161/psb.4.6.8359>.
- Coletta-Filho, H. D., Targon, M. L. P. N., Takita, M. A., De Negri, J. D., Jr, P., & Machado, M. A. (2004). First report of the causal agent of Huanglongbing (“*Candidatus* Liberibacter asiaticus”) in Brazil. *Plant Disease*, 88(12), 2004–2005. <https://doi.org/10.1094/PDIS.2004.88.12.1382C>.
- Cui, W., & Lee, J. Y. (2016). Arabidopsis callose synthases CalS1/8 regulate plasmodesmal permeability during stress. *Nature Plants*, 2(5), 1–9. <https://doi.org/10.1038/NPLANTS.2016.34>.
- Dong, X., Hong, Z., Chatterjee, J., Kim, S., & Verma, D. P. S. (2008). Expression of callose synthase genes and its connection with Npr1 signaling pathway during pathogen infection. *Planta*, 229(1), 87–98. <https://doi.org/10.1007/s00425-008-0812-3>.
- Douglas, C. M., Foor, F., Marrinan, J. A., Morin, N., Nielsen, J. B., Dahl, A. M., et al. (1994). The *Saccharomyces cerevisiae* FKS1 (ETG1) gene encodes an integral membrane protein which is a subunit of 1,3-beta-D-glucan synthase. *Proceedings of the National Academy of Sciences of the United States of America*, 91(26), 12907–12911. <https://doi.org/10.1073/pnas.91.26.12907>.
- Ellinger, D., & Voigt, C. A. (2014). Callose biosynthesis in arabidopsis with a focus on pathogen response: What we have learned within the last decade. *Annals of Botany*, 114(6), 1349–1358. <https://doi.org/10.1093/aob/mcu120>.
- Enns, L. C., Kanaoka, M. M., Torii, K. U., Comai, L., Okada, K., & Cleland, R. E. (2005). Two callose synthases, GSL1 and GSL5, play an essential and redundant role in plant and pollen development and in fertility. *Plant Molecular Biology*, 58(3), 333–349. <https://doi.org/10.1007/s11103-005-4526-7>.
- Etxeberria, E., Gonzalez, P., Achor, D., & Albrigo, G. (2009). Anatomical distribution of abnormally high levels of starch in HLB-affected Valencia orange trees. *Physiological and Molecular Plant Pathology*, 74(1), 76–83. <https://doi.org/10.1016/j.pmpp.2009.09.004>.
- Gómez-Gómez, L., Felix, G., & Boller, T. (1999). A single locus determines sensitivity to bacterial flagellin in *Arabidopsis thaliana*. *Plant Journal*, 18(3), 277–284. <https://doi.org/10.1046/j.1365-313X.1999.00451.x>.
- Grant, M., & Mansfield, J. (1999). Early events in host-pathogen. *Current Opinion in Plant Biology*, 2, 312–319.
- Hong, Z., Delauney, A. J., & Verma, D. P. (2001). A cell plate-specific callose synthase and its interaction with phragmoplastin. *The Plant Cell*, 13(4), 755–768. <https://doi.org/10.1105/tpc.13.4.755>.
- Jacobs, A. K. (2003). An *Arabidopsis* Callose Synthase, GSL5, is required for wound and papillary callose formation. *The Plant Cell Online*, 15(11), 2503–2513. <https://doi.org/10.1105/tpc.016097>.
- Jin, L., & Mackey, D. M. (2017). Measuring callose deposition, an indicator of cell wall reinforcement, during bacterial infection in Arabidopsis. In P. Shan & L. He (Eds.), *Plant Pattern Recognition Receptors*, 1578, 195–205. Springer science-business. <https://doi.org/10.1007/978-1-4939-6859-6>.
- Jones, J. D. G., & Dangl, J. L. (2006). The plant immune system. *Nature*, 444(7117), 323–329. <https://doi.org/10.1038/nature05286>.
- Kim, J.-S., Sagaram, U. S., Burns, J. K., Li, J.-L., & Wang, N. (2009). Response of sweet orange (*Citrus sinensis*) to “*Candidatus* Liberibacter asiaticus” infection: Microscopy and microarray analyses. *Phytopathology*, 99(1), 50–57. <https://doi.org/10.1094/PHYTO-99-1-0050>.
- Koh, E. J., Zhou, L., Williams, D. S., Park, J., Ding, N., Duan, Y. P., & Kang, B. H. (2012). Callose deposition in the phloem plasmodesmata and inhibition of phloem transport in citrus leaves infected with “*Candidatus* Liberibacter asiaticus.” *Protoplasma*, 249(3), 687–697. <https://doi.org/10.1007/s00709-011-0312-3>.
- Kumar, s., Stecher, G., & Tamura, K. (2016). MEGA7: Molecular evolutionary genetics analysis version 7.0 for bigger datasets. *Molecular Biology and Evolution*, 33(7), 1870–1874.
- Lairson, L. L., Henrissat, B., Davies, G. J., & Withers, S. G. (2008). Glycosyltransferases: Structures, functions, and mechanisms. *Annual Review of Biochemistry*, 77(1), 521–555. <https://doi.org/10.1146/annurev.biochem.76.061005.092322>.
- Li, Y., Baldauf, S., Lim, E.-K., & Bowles, D. J. (2001). Phylogenetic analysis of the UDP-glycosyltransferase multigene family of *Arabidopsis thaliana*. *Journal of Biological Chemistry*, 276(6), 4338–4343. <https://doi.org/10.1074/jbc.M007447200>.
- Liao, H. L., & Burns, J. K. (2012). Gene expression in Citrus sinensis fruit tissues harvested from huanglongbing-infected trees: Comparison with girdled fruit. *Journal of Experimental Botany*, 63(8), 3307–3319. <https://doi.org/10.1093/jxb/ers070>.
- Livak, K. J., & Schmittgen, T. D. (2001). Analysis of relative gene expression data using real-time quantitative PCR and. *Methods*, 25, 402–408. <https://doi.org/10.1006/meth.2001.1262>.
- Luna, E., Pastor, V., Robert, J., Flors, V., Mauch-Mani, B., & Ton, J. (2011). Callose deposition: A multifaceted plant defense response. *Molecular Plant-Microbe Interactions*, 24(2), 183–193. <https://doi.org/10.1094/MPMI-07-10-0149>.
- Mafra, V., Kubo, K. S., Alves-Ferreira, M., Ribeiro-Alves, M., Stuart, R. M., Boava, L. P., Rodrigues, C. M., & Machado, M. A. (2012). Reference genes for accurate transcript normalization in citrus genotypes under different experimental conditions. *PLoS One*, 7(2), e31263. <https://doi.org/10.1371/journal.pone.0031263>.
- Murray, M. G., & Thompson, W. F. (1980). Rapid isolation of high molecular weight plant DNA. *Nucleic Acids Research*, 8(19), 4321–4326. <https://doi.org/10.1093/nar/8.19.4321>.
- Nedukha, O. M. (2015). Callose: Localization, functions, and synthesis in plant cells. *Cytology and Genetics*, 49(1), 49–57. <https://doi.org/10.3103/S0095452715010090>.
- Nishimura, M. T. (2008). Loss of a callose synthase results in salicylic acid – Dependent. *Science*, 969(2003), 969–972. <https://doi.org/10.1126/science.1086716>.

- Raffaële, S., Win, J., Cano, L. M., & Kamoun, S. (2010). Analyses of genome architecture and gene expression reveal novel candidate virulence factors in the secretome of *Phytophthora infestans*. *BMC Genomics*, *11*, 637. <https://doi.org/10.1186/1471-2164-11-637>.
- Richmond, T. a., & Somerville, C. R. (2000). The cellulose synthase superfamily. *Plant Physiology*, *124*(2), 495–498. <https://doi.org/10.1104/pp.124.2.495>.
- Scacheri, C. A., & Scacheri, P. C. (2015). Mutations in the non-coding genome. *Current Opinion in Pediatrics*, *27*(6), 659–664. <https://doi.org/10.1097/MOP.0000000000000283>.
- Sievers, F., Wilm, A., Dineen, D., Gibson, T. J., Karplus, K., Li, W., Lopez, R., McWilliam, H., Remmert, M., Soding, J., Thompson, J. D., & Higgins, D. G. (2011). Fast, scalable generation of high-quality protein multiple sequence alignments using Clustal omega. *Molecular Systems Biology*, *7*(539), 539. <https://doi.org/10.1038/msb.2011.75>.
- Sinzelle, L., Izsvák, Z., & Ivics, Z. (2009). Molecular domestication of transposable elements: From detrimental parasites to useful host genes. *Cellular and Molecular Life Sciences*, *66*(6), 1073–1093. <https://doi.org/10.1007/s00018-009-8376-3>.
- Stone, B. A., & Clarke, A. (1992). *Chemistry and Biology of (1–3)-β-D-Glucans*. Victoria: La Trobe University Press.
- van Geest, M., & Lolkema, J. S. (2000). Membrane topology and insertion of membrane proteins: Search for Topogenic signals. *Microbiology and Molecular Biology Reviews*, *64*(1), 13–33. <https://doi.org/10.1128/MMBR.64.1.13-33.2000>.
- Verma, D., & Hong, Z. (2011). Plant callose synthase complexes. *Plant Molecular Biology*, *47*, 693–701. [10.1023/A](https://doi.org/10.1023/A).
- Wang, N., & Trivedi, P. (2013). Citrus Huanglongbing : A newly relevant disease presents unprecedented challenges. *Phytopathology*, *103*(7), 652–665. <https://doi.org/10.1094/PHYTO-12-12-0331-RVW>.
- Wang, N., Pierson, E. A., Setubal, C., Xu, J., Levy, J. G., Zhang, Y., et al. (2017). Liberibacter – Host Interface : Insights into pathogenesis mechanisms and disease control. *Annual Review of Phytopathology*, *55*(June), 1–32. <https://doi.org/10.1146/annurev-phyto-080516-035513>.
- Xie, B., & Hong, Z. (2011). Unplugging the callose plug from sieve pores. *Plant Signaling & Behavior*, *6*(4), 491–493. <https://doi.org/10.4161/psb.6.4.14653>.
- Xie, B., Wang, X., Zhu, M., Zhang, Z., & Hong, Z. (2011). CalS7 encodes a callose synthase responsible for callose deposition in the phloem. *Plant Journal*, *65*(1), 1–14. <https://doi.org/10.1111/j.1365-313X.2010.04399.x>.
- Yu, Y., Jiao, L., Fu, S., Yin, L., Zhang, Y., & Lu, J. (2015). Callose synthase family genes involved in the grapevine defense response to downy mildew disease. *Phytopathology*, *106*(1), 56–64.
- Zou, H., Gowda, S., Zhou, L., Hajeri, S., Chen, G., & Duan, Y. (2012). The destructive Citrus pathogen, “*Candidatus Liberibacter asiaticus*” encodes a functional Flagellin characteristic of a pathogen-associated molecular pattern. *PLoS One*, *7*(9), e46447. <https://doi.org/10.1371/journal.pone.0046447>.